Desalination and Water Treatment
www.deswater.com
doi: 10.5004/dwt.2021.27504

231 (2021) 367–376
August

Adsorption of 4-chloro-2,5-dimethoxyaniline from solution in batch mode using chemical activated pyrolytic char

Haojiang Wang[a], Qiong Liu[b,*], Zhiqiang Wang[a], Runping Han[a,*]

[a]*College of Chemistry, Green Catalysis Center, Zhengzhou University, No. 100 of Kexue Road, Zhengzhou 450001, China, emails: rphan67@zzu.edu.cn (R. Han), wanghaojiang97@163.com (H. Wang), 445876451@qq.com (Z. Wang)*
[b]*School of Environmental Engineering and Chemistry, Luoyang Institute of Science and Technology, No. 90 of Wangcheng Road, Luoyang 471000, China, email: heidy2007@126.com*

Received 24 March 2021; Accepted 10 June 2021

ABSTRACT

In this work, activated pine-sawdust pyrolytic char (APC) was prepared using pine-sawdust pyrolytic char and activated using ammonium phosphate as a chemical agent. The yield of carbon was 72.1%. Characterization of APC was performed such as Fourier-transform infrared spectroscopy, X-ray diffraction and scanning electron microscopy, etc. The adsorption behavior of APC toward 4-chloro-2,5-dimethoxyaniline (CDMA) was studied in batch mode. The results showed that acidity affected adsorption property while ion strength had little effect on adsorption. The maximum adsorption capacity of CDMA onto APC was 134 mg g^{-1} at pH 10, 0.005 g adsorbent dose, 180 min contact time, 80 mg L^{-1} initial concentration at 303 K. There was good efficiency of regeneration using 1% HCl solution and the first time of regeneration rate reached 30.8%. The adsorption was a spontaneous, endothermic process. Koble–Corrigan, Langmuir, pseudo-second-order and Elovich models were suitable to predict the equilibrium and kinetic process. The best fitted were Koble–Corrigan and Elovich models with R^2 value > 0.959 and >0.919, respectively. It was concluded that APC is promising as an alternative to remove CDMA from the solution.

Keywords: Activated pyrolytic char; Adsorption; 4-chloro-2,5-dimethoxyaniline; Regeneration

1. Introduction

As yet, the techniques employed for getting rid of pollutants in sewage include physical technology (adsorption, filtration), chemical (photocatalytic degradation, photo-oxidation) and biological (microbial degradation, aerobic and anaerobic) [1]. Among the methods for the removal of refractory contaminants, adsorption appears to be a good choice in terms of cost and operation for the removal of aniline and its derivatives [2]. Commercial activated carbon adsorption is one of the effective means for advanced treatment of industrial wastewater at present, but its cost is too high and the regeneration of spent activated carbon is relatively difficult. So, the preparation of pyrolytic char into activated pyrolytic char with good adsorption performance is the focus of activated carbon research. Therefore, the development of low-cost adsorbents for wastewater treatment has always been the focus of attention [3–6].

Char proved considerably high adsorption comparable to the activated carbon at different temperatures and pressures [7]. Due to the low cost of char and the large-scale environmental remediation of multiple effects yielded to the receiving environment, char has been widely used in the fields of soil amendment and adsorbent [8]. Biomass pyrolysis is an oxygen-limited thermal degradation process that converts biomass into solid, gas and liquid products. The by-product of this process, pyrolytic char, is different

* Corresponding authors.

from char formed by local combustion. Pyrolytic char can be used directly or simply modified as an adsorbent to remove heavy metal ions and dyes [9,10].

China is a big country of forestry, pine-sawdust as the processed waste of forestry, which can be prepared into pyrolytic char to make full use of the waste. The pyrolytic char has a loose texture, uniform particle and rich carbon content, so it is a good material for preparing highly adsorbed activated carbon. And pyrolytic char products can be prepared by one-step activation. Cheng et al. [11] selected the new pomelo peel char under the condition of high-temperature nitrogen the char was further activated by KOH, which had a larger specific surface area and the maximum adsorption capacity of tetracycline reached 476.19 mg g^{-1}. The research results of Farzad and Robert et al. [12] showed that the morphology and structure of the carbon obtained by pyrolysis is similar to that of natural carbon, and the activated carbon obtained by modification also has developed pore structure and great surface area. Meanwhile, due to the presence of many oxygen-containing functional groups on the surface of carbon, it can be widely used to adsorb a variety of organic compounds in industrial wastewater. Islam et al. [13] used palm leaves as raw materials and sodium hydroxide as the reaction activator. They were first mixed at 200°C for hydrothermal carbonization, and then the product was pyrolyzed at 600°C to produce a specific surface area of 1,233.89 m^2 g^{-1} of activated carbon, the maximum adsorption capacity of methylene blue at 30°C, 40°C, 50°C, are 612.1, 464.3 and 410.0 mg g^{-1}, respectively. Shamik et al. [14] used sodium hydroxide to modify rice husks, and its maximum adsorption capacity for crystal violet was 70.275 mg g^{-1}. Gholamhasan et al. [15] used phosphoric acid to activate lemon peel at a high temperature of 500°C, and its maximum adsorption capacity for rhodamine B and erythrosine B was 296 and 254 mg g^{-1}, respectively. Wang et al. [16] used hydrothermal carbonization of rice husks to prepare carbon fibers with excellent performance, which can be used as a lithium-ion battery material.

In current society, with the rapid development of industry, many emerging contaminants, such as aniline and endocrine disruptors, which cause great harm to the environment, have gradually attracted people's attention [17]. They are very complex toxic organics, usually derived from pharmaceuticals, antibiotics and industrial chemicals, generally present in the water where concentrations are relatively low, but they may have potential impacts on human health after being accumulated by organisms through the food chain [18]. Toxic chemical agents have also endangered the balance of the natural ecosystem due to genotoxic and mutagenic that can cause heritable disorders that may pass to future generations [19].

Aniline is an important chemical intermediate, which is mainly used in pesticides, medicine and dyestuff. It does great harm to the human body, especially to the blood and nerves, and even can lead to cancer [20]. With the development of industry, the demand for aniline will also increase. Aniline-containing wastewater may cause great harm to the environment due to its toxicity and environmental accumulation [21]. How to reduce the harm of aniline to the environment and the human body has important practical significance.

4-chloro-2,5-dimethoxyaniline (CDMA) is an important azo pigment and pesticide intermediate. Because the yield of these intermediates cannot reach 100% in the reaction, some of them will enter the water. In the dying process, 3~5 ton wastewater is produced for every 100 m of fabric, which has become one of the most serious water pollutions, seriously threatening human health and ecosystem [22,23].

The objective is to the preparation of activated pyrolytic char for removal of CDMA from solution. Herein, activated pine-sawdust pyrolytic char (APC) was obtained from pine-sawdust pyrolytic char (PyC) through a novel chemical activation ($(NH_4)_2HPO_4$ as activated agent), which is used for the adsorption of CDMA. The adsorption isotherm of CDMA on APC was obtained and analyzed while the adsorption kinetic data were fitted with a kinetic model. Regeneration of APC was performed also.

2. Materials and methods

2.1. Reagents and materials

Sulfuric acid (H_2SO_4, 95%~98%), hydrochloric acid (HCl, 36%~38%), sodium hydroxide (NaOH, 50%), sodium chloride (NaCl, ≥99.5%), calcium chloride ($CaCl_2$, ≥96.0%), sodium sulfate (Na_2SO_4, ≥99.0%) and ammonium phosphate ($(NH_4)_2HPO_4$, ≥99.0%), 4-chloro-2,5-dimethoxyaniline (CDMA, ≥98%) were all analytical grade chemical from Fucheng Chemical Reagent (Tianjin) and Yongda Co. (Tianjin), that is, and could be used without further purification. Pine-sawdust pyrolytic char (PyC) was obtained from the Research Institute of Environmental Sciences, Zhengzhou University. It was produced by slow pyrolysis of biomass in a fluidized reactor to obtain pyrolytic oil.

2.2. Preparation of APC

Deionized water was used to clean the solid residue repeatedly after pyrolysis to remove the mixed floating objects. It was sieved to a particle size (80–100 mesh) and collected after drying to constant weight at 50–60°C. 0.1 g PyC was weighed into the crucible and soaked in a certain volume of $(NH_4)_2HPO_4$ solution for 24 h before being placed in a box-type resistance furnace. The temperature was controlled at 450°C and heated for 1 h in the N_2 atmosphere. The crude products were first pickled with 10% hydrochloric acid solution in a 90°C water bath for 1 h, and then washed to neutral with distilled water. After extraction, it dried to constant weight for collection at 50°C–60°C.

2.3. Characterization of PyC and APC

The qualitative and semi-quantitative analyses of the chemical groups on the surface of the two materials were analyzed by Fourier-transform infrared spectrometer (FTIR, PE-1710, USA) in the range of wavenumber is 400~4,000 cm^{-1}. Boehm titration was used to determine the amount of surface acidic and basic functional groups. Scanning electron microscopy (SEM, JSM-6700F, Japan) was adopted to observe the morphology of PyC and APC. The X-ray diffractometer could be employed the effectively crystallographic structure of PyC and APC in an angle range

of 0°–80° X-ray diffraction (XRD, D-Max RA, Japan). The element content of the two materials was determined by Elemental Analyzer (Flash EA 1112, USA). The N_2 adsorption–desorption was used for specific surface area analysis Brunauer–Emmett–Teller (BET, NOVA l000e, USA).

2.4. Adsorption experiments

Adsorption tests were carried out in one rotary shaker at 100 rpm using 50 mL shake flasks containing 20 mL of known CDMA concentrations with 0.010 g of APC. The effects of APC pH, ion strength, time, equilibrium concentration and other factors on the adsorption effect were investigated in batch mode. The unit adsorption amount of APC during the adsorption process was calculated using the following equation [24].

$$q = \frac{V\left(C_0 - C\right)}{m} \tag{1}$$

where q (mg g^{-1}) is the adsorption quantity, C_0 (mg L^{-1}) is the initial CDMA concentration, C (mg L^{-1}) is the CDMA concentration at any time t or equilibrium (mg L^{-1}), V (L) is the CDMA solution volume, and m (g) is the mass of APC.

2.5. Desorption and regeneration experiments

To assess the reusability of APC, the regeneration of CDMA-loaded APC and reuse were conducted for three consecutive cycles. Desorption and regeneration experiments of APC were carried out at 303 K by various methods. Including acid (HCl) bubble, alkali (NaOH) bubble, distilled water. After desorption of APC was collected and dried, CDMA was performed multiple desorption cycle experiments under the same conditions. After a comprehensive comparison, the best desorption method was selected to investigate whether APC could be used for multiple cycles. The desorption efficiency and regeneration efficiency were calculated by the following.

$$d = \frac{m_d}{m_0} \times 100\% \tag{2}$$

$$r = \frac{q_n}{q_0} \times 100\% \tag{3}$$

where d (%) is the desorption efficiency of the adsorbent, m_d is the CDMA mass (g), which is desorbed from the adsorbent, m_0 is the mass that adsorbate is remaining on the adsorbent before desorption; η (%) is regeneration efficiency of the adsorbent, q_0 (mg g^{-1}) is the unit adsorption amount of the first adsorption equilibrium, q_n (mg g^{-1}) is the unit adsorption amount, n is the number of regeneration times.

3. Results and discussion

3.1. Characterization of PyC and APC

3.1.1. FTIR analysis

The FTIR of PyC and APC materials is shown in Fig. 1. It was found that there was no change in the FTIR after modification. The stretching vibration absorption peaks at 3,439 and 3,423 cm^{-1} represented –OH, and the absorption peaks near 1,600 cm^{-1} could be attributed to the bending vibration absorption of O–H bond in pyrolytic char [6]. This –OH might come from the stretching vibrations of –OH, –COOH and the hydroxyl group in the water of chemical adsorption on the carbon surface. After modification, the peak strength decreased, indicating that the amount of –OH decreased. The peak at 2,924 cm^{-1} was due to symmetric

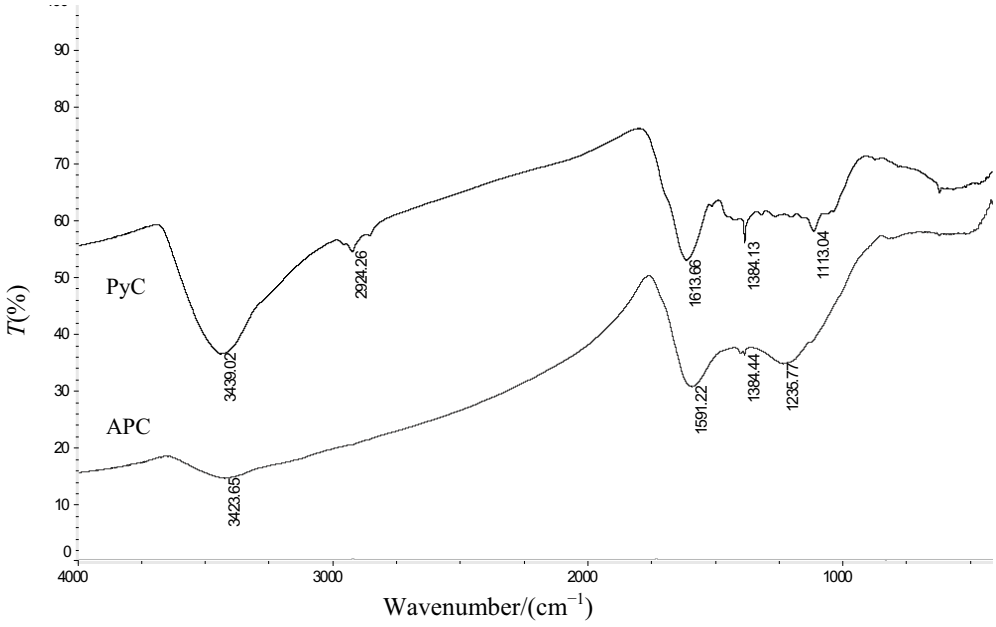

Fig. 1. FTIR spectra of PyC and APC.

(and antisymmetric) stretching vibration of $–CH_2–$, $–CH_3$ and –CH– while the absorption at 1,384 cm^{-1} was ascribed to symmetric deformation vibration of C–H bonds [25]. Peaks near 1,116 and 1,236 cm^{-1} might correspond to symmetric and asymmetric C–O vibrations, which could be attributed to the C–O stretching vibration in –O–CH– [9].

3.1.2. Boehm titration and elemental analysis

The ash content of PyC was 13.8%, indicating that the carbon content was high. So PyC with high carbon content was more beneficial to be modified into activated carbon with high adsorption capacity. The yield of APC is 72.1%.

X-ray fluorescence analysis presented that the phosphorus and chlorine elements in APC were higher, and the content of calcium was lower; conversely, phosphorus and chlorine were not detected for PyC. The reason was PyC was activated to acquire APC by $(NH_4)_2HPO_4$ and eluted with HCl. The amount of carboxyl and lactonic groups on the surface of APC increased significantly (from 0.608 to 1.31 mmol g^{-1} for carboxyl and from 0.282 to 0.544 mmol g^{-1} for lactonic) and indicated that activation facilitated the generation of acidity on the surface of PyC, resulting in an increased number of acidic groups, and the result was consistent with lower pH_{pzc} value of APC.

The element contents of PyC were C 65.2%, H 3.39% and N 0.0207%; on the contrary, the contents of elemental analysis were C 55.3%, H 2.57% and N 5.03% for APC. The elemental analysis indicated that the contents of C, H became less after activation, and N became higher remarkably because of $(NH_4)_2HPO_4$ as an activated agent. In addition, according to TG analysis, the PyC carbonization process was quite intense, with a weight loss of 17.72%, since APC had been heated and activated, so its relative weightlessness was relatively small, with a weightlessness rate of 7.49%.

3.1.3. Nitrogen adsorption and desorption

The specific surface area is one of the important factors affecting the adsorption capacity of adsorbent and the BET method was used to obtain the specific surface area of PyC and APC. Fig. 2a and b are isotherm and aperture distribution diagrams of PyC and APC's absorption and desorption of N_2, respectively.

The surface area of PyC and APC were 0.52 and 407.3 $m^2\ g^{-1}$, respectively. The result illustrated that the surface area of PyC was conspicuously increased after activation. Fig. 2b shows the pore-size distribution of PyC and APC, and the average radius of the pore was 29.8 and 2.08 nm, respectively. The pore size of APC has decreased significantly, indicating that it contains a large number of new microporous and mesoporous, which obviously increased the surface area and adsorption capacity [26–29].

3.1.4. XRD analysis

The microcrystalline structure of materials can be studied effectively by X-ray diffraction. The XRD patterns of PyC and APC are shown in Fig. 3. It shows a primary peak near 23°~24° and a secondary peak at 42°. These represented the characteristic diffraction peaks of the microcrystalline (002) and (100) crystal planes in graphite-like structures, respectively. The very wide diffraction peaks

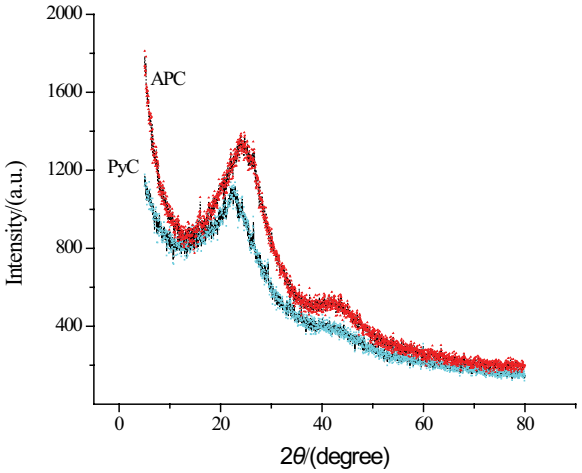

Fig. 3. XRD pattern of PyC and APC.

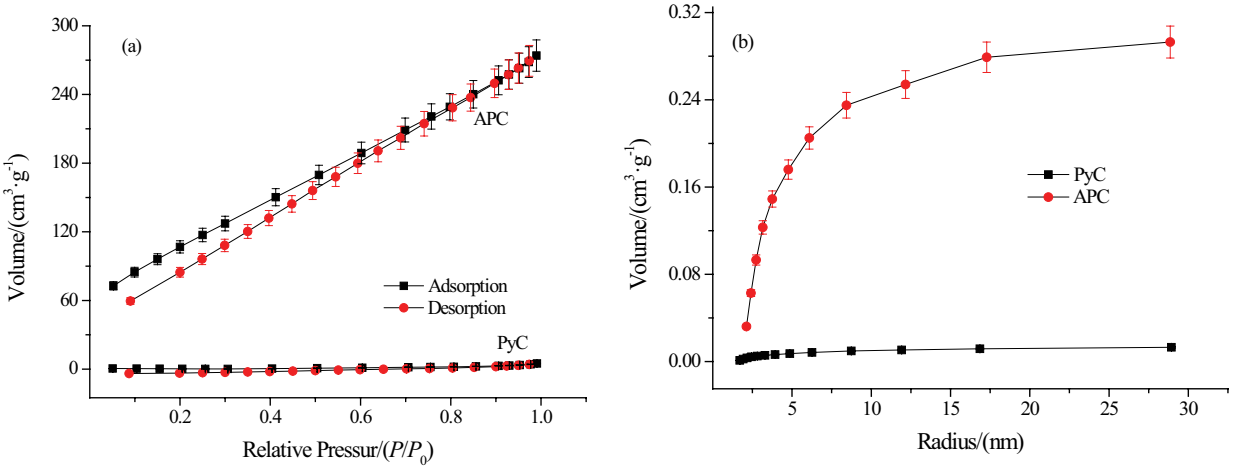

Fig. 2. (a) Nitrogen adsorption and desorption and (b) pore-size distribution of PyC and APC.

indicated the amorphous structure formed. The APC's peak was stronger than the PyC, indicating that it developed in an orderly direction.

3.1.5. SEM analysis

Fig. 4 shows the SEM images of PyC and APC at 2,000 times magnification. It could be clearly found that the surface of PyC was rough, with many small irregular-shaped particles, which blocked the pores [30]. After modification, the impurities were removed, and the surface was smooth and developed, but there was no fixed shape, which verifies the disordered result of XRD.

3.2. Batch adsorption studies

3.2.1. Effect of pH on adsorption

The pH value in the reaction is an essential ingredient for the adsorption property as it can affect the surface binding sites and the protonation of functional groups. The effect of pH on adsorption is illustrated in Fig. 5, which shows that values of q_e changed with solution pH from 2 to 12. In the range of pH from 4 to 11, the pH has little effect on the unit adsorption capacity. Since the isoelectric point of pine-sawdust pyrolytic char before and after the medication was reduced from 6.75 to 4.50, which indicated the acidic groups on the surface of pyrolytic char increase after modification, it was beneficial to the adsorption of organic and cations. Similar results were observed about activated pyrolytic char using a chemical agent and microwave irradiation for removal of 4-chloro-2,5-dimethoxy nitrobenzene from solution [9].

When the pH < pH_{pzc} (zero point of charge), the APC surface attracted protons and carried positive charges, which was not conducive to the adsorption of cations in the solution. When the pH > pH_{pzc}, the surface of the adsorbent released protons and carried negative charges, which was beneficial to the adsorption of CDMA [29]. Nevertheless, in Fig. 5, at solution pH less than 7, the adsorption capacity was still very formidable, indicating that the electrostatic effect had a weaker effect on the adsorption capacity.

3.2.2. Effect of salt concentration on adsorption

There are many coexisting ions in the actual wastewater, which have a great influence on the adsorption quantity. Fig. 6 reveals that when NaCl and Na_2SO_4 were presented in the adsorbents, the unit adsorption capacity of APC decreased. With the increase of sodium concentration, the unit adsorption capacity of APC decreased gradually to no change. Na_2SO_4 had a greater influence on the APC adsorption CDMA process because its ionic strength was greater than NaCl. In the presence of Na^+, it might compete with CDMA and occupied the active site of APC, leading to a slight decrease in the adsorption capacity of APC.

3.2.3. Adsorption isotherm study

The effect of the equilibrium concentration of solution at various temperatures on adsorption is shown in Fig. 7 (adsorption isotherm). It was clearly seen that as the equilibrium concentration of CDMA increased, the adsorption capacity also gradually increased. The reason was driving force of the concentration gradient was enhanced.

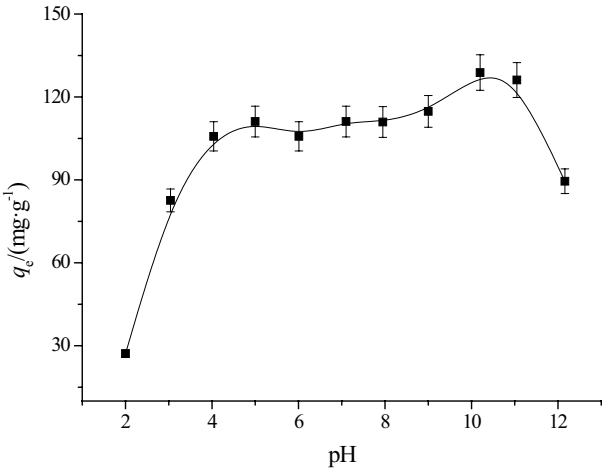

Fig. 5. Effect of solution pH on adsorption.

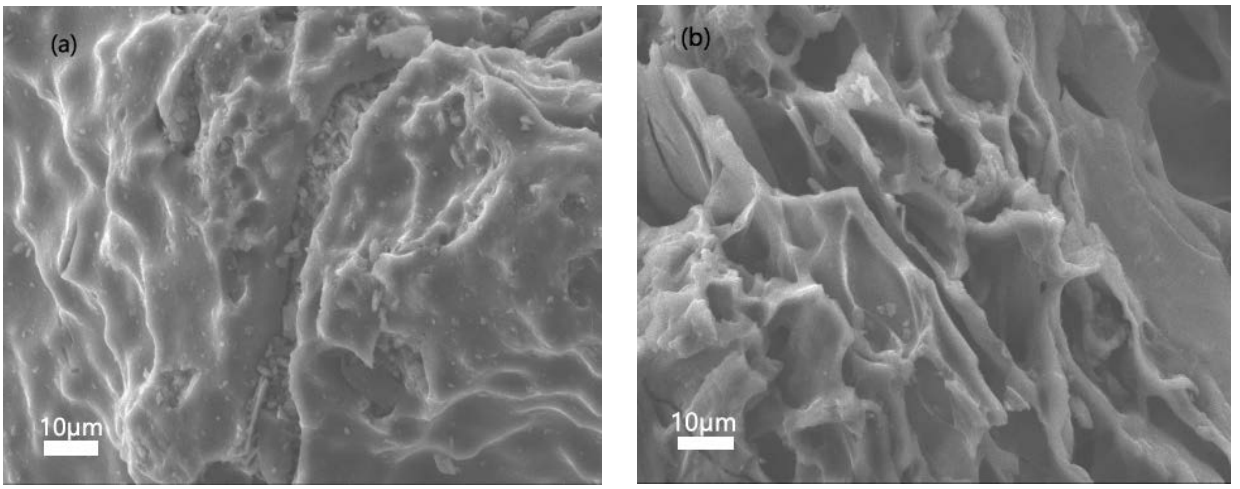

Fig. 4. SEM of PyC (a) and APC (b).

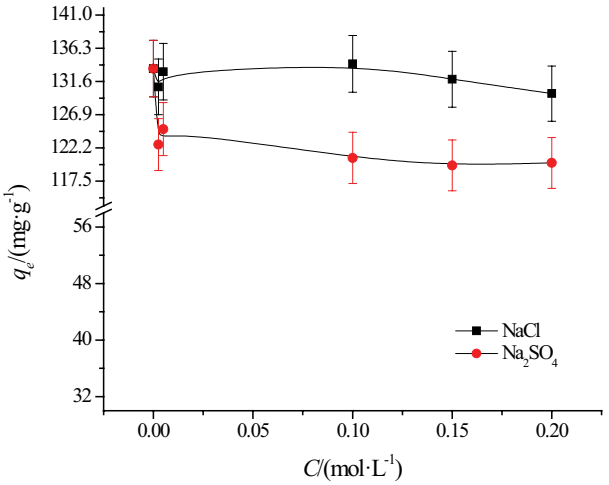

Fig. 6. Effect of salt concentration on adsorption.

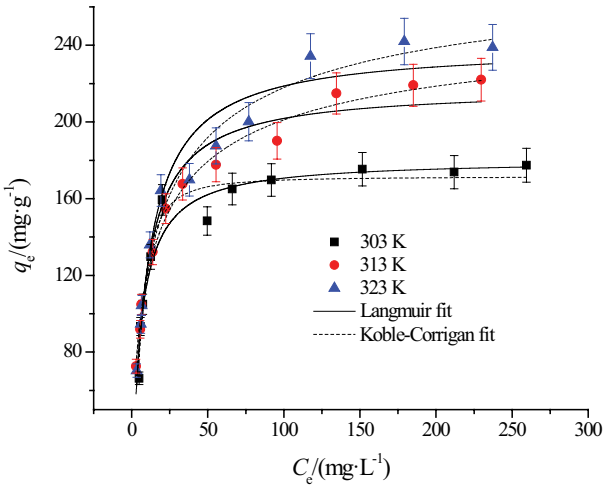

Fig. 7. Adsorption isotherms of CDMA onto APC at various temperatures.

The adsorption capacity of APC for CDMA were 176, 220, and 238 mg g^{-1} at 303, 313 and 323 K, respectively. This might be due to the increase of the concentration, which empowered more adsorbates bound to active sites. What's more, at the initial concentration, the adsorption capacity improved with the ascending solution temperature, which represented that the adsorption process was an endothermic reaction.

Langmuir and Koble–Corrigan models (Table 1) were used to fit the adsorption results using nonlinear regression analysis, and the consequences by R^2 and sum of the squares of errors (SSE) were analyzed. Table 2 displays the fitting results and compares the data of the two models.

As we know, the binding of adsorbate and adsorbent are reacted by K_L, and it is observed from Table 2 that K_L values gradually decreased and q_m saturation adsorption capacity gradually increased with the rise of temperature, indicating that the increase of temperature was conducive to the adsorption of CDMA by APC, but the binding force might be weakened. Thus, although the value of q_m obtained from Langmuir was close to the value of q_e, it is distinctly seen from Table 2 that the Koble–Corrigan model was better described the adsorption of CDMA as there were higher values of R^2 and lower values of SSE.

3.2.4. Adsorption kinetic study

Experiments observed that there was almost adsorption capacity about PyC toward CDMA (q_e = 1.5 mg g^{-1}), while the unit adsorption capacity of CDMA by APC reached 120 mg g^{-1} at same condition, and the adsorption ability was increased by 100 times, indicating that the adsorption capacity was impressively increased after activation. Fig. 8 shows the effect of contact time on the adsorption capacity at three initial concentrations and different temperatures. As the concentration of the solution increased, the equilibrium adsorption quantity gradually enhanced. In addition, the pseudo-second-order and Elovich models (Table 1) were used to fit experimental data to forecast the adsorption mechanism of CDMA by APC. The fitted data are listed in Table 3.

Table 1
Adsorption isotherms and kinetic models

Model name	Expression	Parameter
Langmuir model	$q_e = \frac{q_m K_L c_e}{1 + K_L c_e}$	q_m (mg g^{-1}) is the saturated adsorption amount; K_L (L mg^{-1}) is a constant related to the binding energy
Koble–Corrigan model	$q_e = \frac{AC_e^n}{1 + BC_e^n}$	A, B, and n are the Koble–Corrigan isotherm constants
Pseudo-second-order kinetic model	$q_t = \frac{k_2 q_e^2 t}{1 + k_2 q_e t}$	q_t is adsorption quantity at time (t); k_2 (g mg^{-1} min^{-1}) is the rate constant of the equation
Elovich equation	$q_t = \frac{\ln(a\beta)}{\beta} + \frac{\ln t}{\beta}$	α (g mg^{-1} min^{-1}) is the initial adsorption rate constant; β (g mg^{-1}) is related to the extent of surface coverage and activation energy for chemisorption

Table 2
Parameters of adsorption isotherm models for APC adsorption onto CDMA

Langmuir model					
T (K)	$q_{e(\exp)}$ (mg g^{-1})	$q_{m(\text{theo})}$ (mg g^{-1})	K_L (L mg^{-1})	R^2	SSE
303	176	180	0.178	0.941	0.869
313	220	218	0.127	0.962	1.04
323	238	240	0.105	0.959	1.50
Koble–Corrigan model					
T (K)	A	B	n	R^2	SSE
303	10.8	0.0632	1.59	0.959	0.604
313	54.8	0.208	5.94	0.992	0.229
323	48.0	0.166	0.633	0.979	0.752

Note: SSE = $\sum\left(q-q_c\right)^2$, q and q_c are the experimental value and calculated value according to the model, respectively.

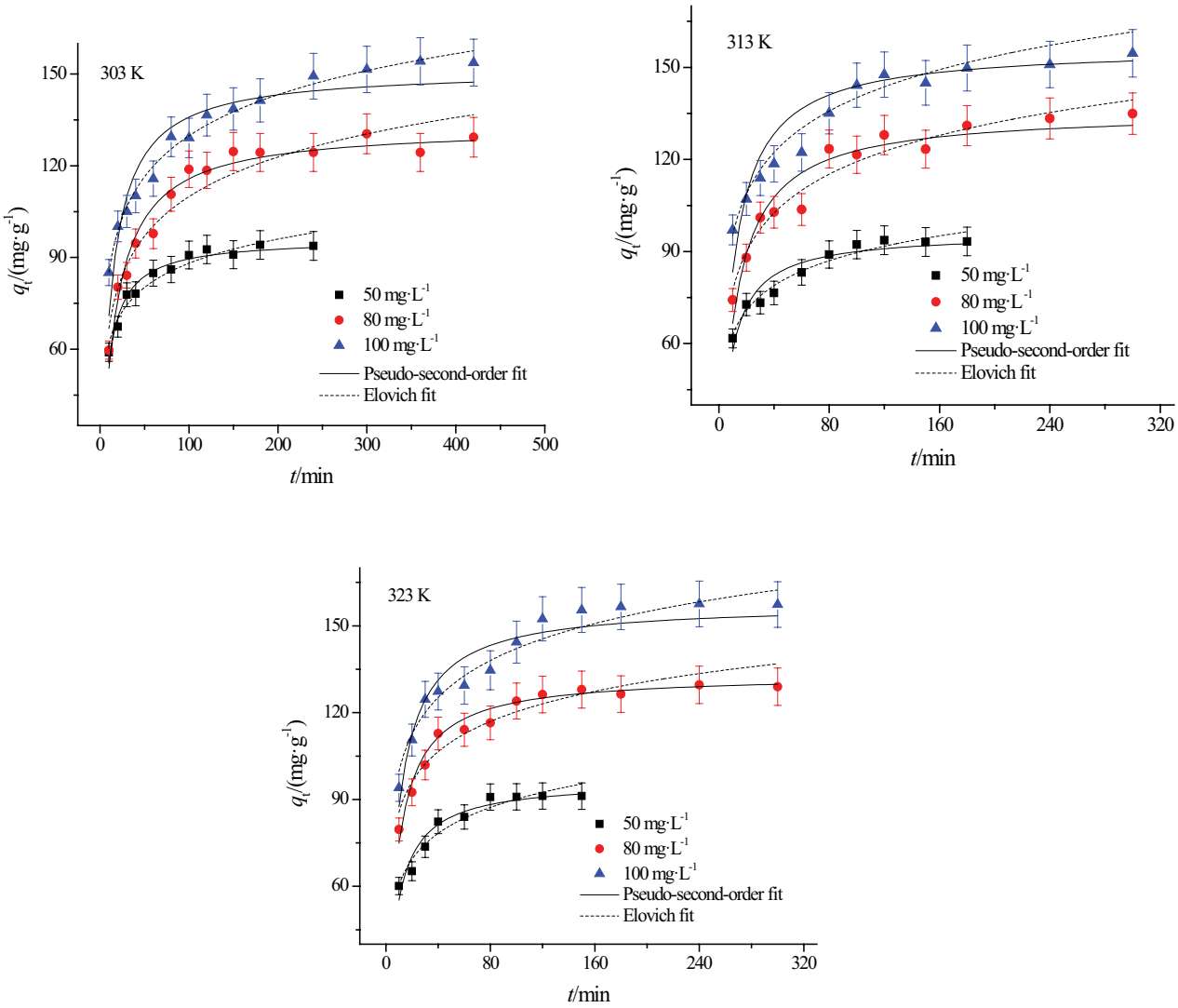

Fig. 8. Effect of contact time on the adsorption at various initial concentrations.

Table 3
Parameters of kinetic models for CDMA adsorption onto APC

Pseudo-second-order kinetic model						
T (K)	C_0 (mg L^{-1})	$q_{e(exp)}$ (mg g^{-1})	$q_{e(theo)}$ (mg g^{-1})	k_2	R^2	SSE
303	50	93.5	96.1	1.42	0.966	2.38
	80	124	133	0.510	0.966	8.31
	100	151	151	0.580	0.898	9.31
313	50	93.3	96.0	1.56	0.890	2.17
	80	133	136	0.710	0.930	6.67
	100	154	156	0.730	0.850	7.79
323	50	91.9	96.5	1.39	0.908	2.43
	80	127	133	0.970	0.955	4.83
	100	158	158	0.790	0.885	7.09
Elovich equation						
T (K)	C_0 (mg L^{-1})	α (g mg^{-1} min^{-1})	β (g mg^{-1})		R^2	SSE
303	50	35.6	11.4		0.949	68.8
	80	23.9	18.7		0.933	416
	100	40.5	19.4		0.988	75.0
313	50	35.8	11.7		0.920	93.9
	80	35.0	18.3		0.952	202
	100	50.4	19.5		0.919	400
323	50	30.5	12.9		0.898	122
	80	51.0	15.1		0.895	318
	100	57.3	18.4		0.879	558

It is found from Table 3 that the experimental data had a high degree of fit with the Elovich model, indicating that the adsorption process of APC to CDMA was a heterogeneous process. Moreover, the value of R^2 obtained from the pseudo-second-order kinetic model was also higher. The value of q_e from model was close to that from experiment, and the error was relatively small, indicating that the pseudo-second-order kinetic model also could be described this adsorption process [21]. This showed that there was chemical adsorption between APC and CDMA.

3.3. Thermodynamic parameters of adsorption

The study of thermodynamic analysis can figure out the extent and driving force of adsorption process. Thermodynamic parameters, the free energy change (ΔG°), enthalpy change (ΔH°), entropy change (ΔS°), and activation energy (E_a) were defined as [31].

$$K_c = \frac{C_{ad,c}}{C_e} \tag{4}$$

$$\Delta G^\circ = -RT\ln K_c \tag{5}$$

$$\Delta G^\circ = \Delta H^\circ - T\Delta S^\circ \tag{6}$$

$$\ln k_2 = -\frac{E_a}{RT} + \ln A \tag{7}$$

where K_c is the distribution coefficient for the adsorption, $C_{ad,c}$ is the concentration of CDMA on the adsorbent at equilibrium (mg L^{-1}), R (8.314 J mol^{-1} K^{-1}) the universal gas constant, T temperature (K), and E_a is the apparent activation energy, A (g mg^{-1} min^{-1}) is the temperature-independent factor, When lnk_2 is plotted vs. 1/T, a straight line with slope $-E_a/R$ is obtained [32].

The relevant thermodynamic parameters for the adsorption of CDMA onto APC are shown in Table 4. The following conclusions could be drawn from Table 4: The value of ΔG° decreased from −4.98 to −5.00 kJ mol^{-1} with ascending temperature, and the value of ΔH° was 4.56 kJ mol^{-1}, which indicated that the process of APC adsorbing CDMA was a spontaneous, endothermic process, and raised temperature was beneficial to this reaction. The value of E_a was 4.55 kJ mol^{-1}, indicating that the adsorption process was physical adsorption. The value of ΔS° closed to zero, representing that chaos in the adsorption process of APC for CDMA had not changed.

Table 4
Thermodynamic parameters of APC adsorption on CDMA

E_a	ΔH°	ΔS°	ΔG° (kJ mol^{-1})		
(kJ mol^{-1})	(kJ mol^{-1})	(J mol^{-1} K^{-1})	303 K	313 K	323 K
4.55	4.56	1.40	−4.98	−4.96	−5.00

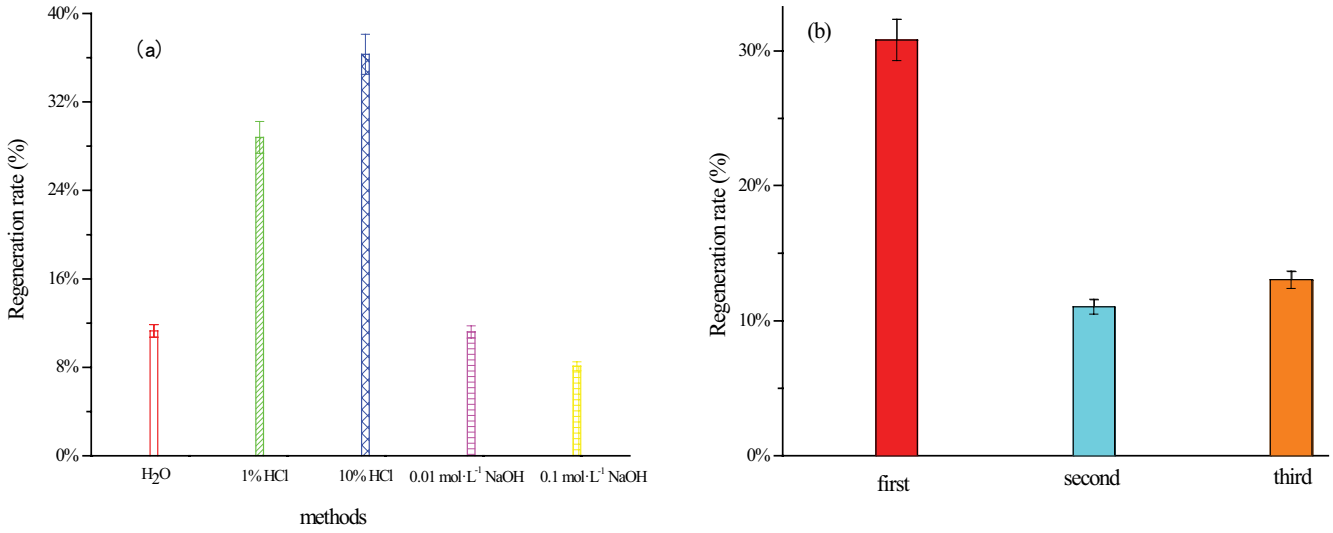

Fig. 9. Regeneration efficiency of various methods (a) and the three regeneration efficiency of selecting 1% HCl (b).

Linked with kinetic analysis, the adsorption of CDMA by APC was inferred as physical adsorption accompanied by chemical adsorption.

3.4. Regeneration study

Regeneration of saturated adsorbents was vital to estimate the reusability of the adsorbents and to clarify the mechanism of adsorption [33–36]. The results of regeneration are shown in Fig. 9.

Among the five methods, the regeneration efficiency of the HCl solution was better. Therefore, select 1% HCl to regenerate the CDMA adsorbed on the APC by three times. The regeneration efficiency of the three cycles was 30.8%, 11%, 13%, respectively. It might be because of the high solubility of CDMA in the HCl, the CDMA onto the APC was easily eluted, and there were many active sites that could be re-adsorbed, leading to a higher regeneration rate than other methods.

4. Conclusion

The adsorption capacity of PyC can be enhanced after activation. The results showed that pH, contact time, adsorbent concentration, salt concentration factors had an influence on CDMA adsorption. The adsorption behavior of APC on CDMA was in line with the Koble–Corrigan model. The effect of contact time at various initial concentrations and different temperatures on adsorption could be described by pseudo-second-order and Elovich models. Adsorption was a spontaneous endothermic process, including the physical and chemical adsorption process. There was some property of regeneration about spent adsorbent. The research on the industrial wastewater treatment of CDMA production showed that The APC adsorption technology could be effectively applied to the industrial wastewater treatment of CDMA production, and had high use value and environmental protection value.

Acknowledgments

This work was financially supported by the Henan province basis and advancing technology research project (142300410224) and Educational Department of Henan Province (13A150650).

References

[1] F.M. Mpatani, A.A. Aryee, A.N. Kani, R.P. Han, Z.H. Li, E. Dovi, L.B. Qu, A review of treatment techniques applied for selective removal of emerging pollutant-trimethoprim from aqueous systems, J. Cleaner Prod., 308 (2021) 127359, doi: 10.1016/j.jclepro.2021.127359.
[2] I. Ali, M. Asim, T.A. Khan, Low cost adsorbents for the removal of organic pollutants from wastewater, J. Environ. Manage., 113 (2012) 170–183.
[3] X. Xu, B.Y. Gao, B. Jin, Q.Y. Yue, Removal of anionic pollutants from liquids by biomass materials: a review, J. Mol. Liq., 215 (2016) 565–595.
[4] Y.L. Liu, X.R. Zhao, J.L. Li, D. Ma, R.P. Han, Characterization of bio-char from pyrolysis of wheat straw and its evaluation on methylene blue adsorption, Desal. Water Treat., 46 (2012) 115–123.
[5] H.N. Bhatti, Z. Mahmood, A. Kausar, S.M. Yakout, O.H. Shair, M. Iqbal, Biocomposites of polypyrrole, polyaniline and sodium alginate with cellulosic biomass: adsorption–desorption, kinetics and thermodynamic studies for the removal of 2,4-dichlorophenol, Int. J. Biol. Macromol., 153 (2020) 146–157.
[6] D. Mohan, S. Rajput, V.K. Singh, P.H. Steele, C.U. Pittman, Jr., Modeling and evaluation of chromium remediation from water using low cost bio-char, a green adsorbent, J. Hazard. Mater., 188 (2011) 319–33.
[7] Z.R. Niu, W.L. Feng, H. Huang, B. Wang, L. Chen, Y.B. Miao, S. Su, Green synthesis of a novel Mn-Zn ferrite/biochar composite from waste batteries and pine sawdust for Pb^{2+} removal, Chemosphere, 252 (2020) 126529, doi: 10.1016/j.chemosphere.2020.126529.
[8] W.-H. Huang, D.-J. Lee, C.P. Huang, Modification on biochars for applications: a research update, Bioresour. Technol., 319 (2021) 124100, doi: 10.1016/j.biortech.2020.124100.
[9] Y.B. Jiao, D.L. Han, Y.Z. Lu, Y.C. Rong, L.Y. Fang, Y.L. Liu, R.P. Han, Characterization of pine-sawdust pyrolytic char activated by phosphoric acid through microwave irradiation

and adsorption property toward CDNB in batch mode, Desal. Water Treat., 77 (2017) 247–255.
[10] A.L. Zhang, X. Li, J. Xing, G.R. Xu, Adsorption of potentially toxic elements in water by modified biochar: a review, J. Environ. Chem. Eng., 8 (2020) 104196, doi: 10.1016/j.jece.2020.104196.
[11] D. Cheng, H.H. Ngo, W. Guo, S.W. Chang, D.D. Nguyen, X.B. Zhang, S. Varjani, Y. Liu, Feasibility study on a new pomelo peel derived biochar for tetracycline antibiotics removal in swine wastewater, Sci. Total Environ., 720 (2020) 137662, doi: 10.1016/j.scitotenv.2020.137662.
[12] S. Farzad, H. Robert, Recent applications in analytical thermochemolysis, J. Anal. Appl. Pyrolysis, 89 (2010) 2–16.
[13] M.A. Islam, I.A.W. Tan, A. Benhouria, M. Asif, B.H. Hameed, Mesoporous and adsorptive properties of palm date seed activated carbon prepared via sequential hydrothermal carbonization and sodium hydroxide activation, Chem. Eng. J., 270 (2015) 187–195.
[14] C. Shamik, C. Sagnik, D.S. Papita, Response surface optimization of a dynamic dye adsorption process: a case study of crystal violet adsorption onto NaOH-modified rice husk, Environ. Sci. Pollut. Res., 20 (2013) 1698–1705.
[15] S. Gholamhasan, A. Alireza, R. Maryam, Highly effective adsorption of xanthene dyes (rhodamine B and erythrosine B) from aqueous solutions onto lemon citrus peel active carbon: characterization, resolving analysis, optimization and mechanistic studies, RSC Adv., 7 (2017) 5362–5371.
[16] L.P. Wang, Z. Schnepp, M.M. Titirici, Rice husk-derived carbon anodes for lithium ion batteries, J. Mater. Chem. A, 1 (2013) 5269–5273.
[17] N. Cheng, B. Wang, P. Wu, X. Lee, Y. Xing, M. Chen, B. Gao, Adsorption of emerging contaminants from water and wastewater by modified char: a review, Environ. Pollut., 273 (2021) 116448, doi: 10.1016/j.envpol.2021.116448.
[18] A.R. Gomes, C. Justino, T. Rocha-Santos, A.C. Freitas, A.C. Duarte, R. Pereira, Review of the ecotoxicological effects of emerging contaminants to soil biota, J. Environ. Sci. Health. Part A Toxic/Hazard. Subst. Environ. Eng., 52 (2017) 992–1007.
[19] M. Iqbal, *Vicia faba* bioassay for environmental toxicity monitoring: a review, Chemosphere, 144 (2016) 785–802.
[20] Y. Zhang, H.J. Li, M.C. Li, M.H. Xin, Adsorption of aniline on aminated chitosan/graphene oxide composite material, J. Mol. Struct., 1209 (2020) 127973, doi: 10.1016/j.molstruc.2020.127973.
[21] D.-W. Gao, Q. Hu, H.Y. Pan, J.P. Jiang, P. Wang, High-capacity adsorption of aniline using surface modification of lignocellulose-biomass jute fibers, Bioresour. Technol., 193 (2015) 507–512.
[22] J.-W. Lee, S.-P. Choi, R. Thiruvenkatachari, W.-G. Shim, H. Moon, Evaluation of the performance of adsorption and coagulation processes for the maximum removal of reactive dyes, Dyes Pigm., 69 (2006) 196–203.
[23] M. Rafatullah, O. Sulaiman, R. Hashim, A. Ahmad, Adsorption of methylene blue on low-cost adsorbents: a review, J. Hazard. Mater., 177 (2010) 70–80.
[24] K. Wen, Y. Li, S. Zhang, X.T. Zhang, R.P. Han, Adsorption of Congo Red from solution by iron doped PVA-chitosan composite film, Desal. Water Treat., 187 (2020) 378–389.
[25] D.A. Jones, T.P. Lelyveld, S.D. Mavrofidis, S.W. Kingman, N.J. Miles, Microwave heating applications in environmental engineering—a review, Resour. Conserv. Recycl., 34 (2002) 75–90.
[26] J. Pastor-Villegas C.J. Durán-Valle, Pore structure of activated carbons prepared by carbon dioxide and steam activation at different temperatures from extracted rockrose, Carbon, 40 (2002) 397–402.
[27] T.Y. Shim, J. Yoo, C.K. Ryu, Y.-K. Park, J.H. Jung, Effect of steam activation of biochar produced from a giant *Miscanthus* on copper sorption and toxicity, Bioresour. Technol., 197 (2015) 85–90.
[28] L.C. Cao, I.K.M. Yu, D.C.W. Tsang, S.C. Zhang, Y.S. Ok, E.E. Kwon, H.C. Song, C.S. Poon, Phosphoric acid-activated wood biochar for catalytic conversion of starch-rich food waste into glucose and 5-hydroxymethylfurfural, Bioresour. Technol., 267 (2018) 242–248.
[29] J.W. Fu, Z.H. Chen, M.H. Wang, S.J. Liu, J.H. Zhang, J.N. Zhang, R.P. Han, Q. Xu, Adsorption of methylene blue by a high-efficiency adsorbent (polydopamine microspheres): kinetics, isotherm, thermodynamics and mechanism analysis, Chem. Eng. J., 259 (2015) 53–61.
[30] Y.M. Awad, Y.S. Ok, J. Abrigata, J. Beiyuan, F. Beckers, D.C.W. Tsang, J. Rinklebe, Pine sawdust biomass and biochars at different pyrolysis temperatures change soil redox processes, Sci. Total Environ., 625 (2018) 147–154.
[31] M.A.K.M. Hanafiah, W.S.W. Ngah, S.H. Zolkafly, L.C. Teong, Z.A.A. Majid, Acid Blue 25 adsorption on base treated *Shorea dasyphylla* sawdust: kinetic, isotherm, thermodynamic and spectroscopic analysis, J. Environ. Sci., 24 (2012) 261–268.
[32] S.S. Chen, Z.Y. Zang, S.S. Zhang, G.F. Ouyang, R.P. Han, Preparation of MIL-100(Fe) and multi-walled carbon nanotubes nanocomposite with high adsorption capacity towards Oxytetracycline from solution, J. Environ. Chem. Eng., 9 (2021) 104780, doi: 10.1016/j.jece.2020.104780.
[33] B.L. Zhao, W. Xiao, Y. Shang, H.M. Zhu, R.P. Han, Adsorption of light green anionic dye using cationic surfactant-modified peanut husk in batch mode, Arabian J. Chem., 10 (2017) S3595–S3602.
[34] F. Ishtiaq, H.N. Bhatti, A. Khan, M. Iqbal, A. Kausar, Polypyrole, polyaniline and sodium alginate biocomposites and adsorption–desorption efficiency for imidacloprid insecticide, Int. J. Biol. Macromol., 147 (2020) 217–232.
[35] A.A. Aryee, F.M. Mpatani, A.N. Kani, E. Dovi, R.P. Han, Z.H. Li, L.B. Qu, A review on functionalized adsorbents based on peanut husk for the sequestration of pollutants in wastewater: modification methods and adsorption study, J. Cleaner Prod., 310 (2021) 127502, doi: 10.1016/j.jclepro.2021.127502.
[36] A. Kausar, M. Iqbal, A. Javed, K. Aftab, Z. Nazli, H.N. Bhatti, S. Nouren, Dyes adsorption using clay and modified clay: a review, J. Mol. Liq., 256 (2018) 395–407.